

# Fractal dimension of domain walls in two-dimensional Ising spin glasses

O. Melchert<sup>1</sup> and A. K. Hartmann<sup>2</sup>

<sup>1</sup>*Institut für Theoretische Physik, Universität Göttingen, 37077 Göttingen, Germany*

<sup>2</sup>*Institut für Physik, Universität Oldenburg, 26111 Oldenburg, Germany*

(Dated: November 13, 2018)

We study domain walls in 2d Ising spin glasses in terms of a minimum-weight path problem. Using this approach, large systems can be treated exactly. Our focus is on the fractal dimension  $d_f$  of domain walls, which describes via  $\langle \ell \rangle \sim L^{d_f}$  the growth of the average domain-wall length with systems size  $L \times L$ . Exploring systems up to  $L = 320$  we yield  $d_f = 1.274(2)$  for the case of Gaussian disorder, i.e. a much higher accuracy compared to previous studies. For the case of bimodal disorder, where many equivalent domain walls exist due to the degeneracy of this model, we obtain a true lower bound  $d_f = 1.095(2)$  and a (lower) estimate  $d_f = 1.395(3)$  as upper bound. Furthermore, we study the distributions of the domain-wall lengths. Their scaling with system size can be described also only by the exponent  $d_f$ , i.e. the distributions are monofractal. Finally, we investigate the growth of the domain-wall width with system size (“roughness”) and find a linear behavior.

PACS numbers: 75.50.Lk, 02.60.Pn, 75.40.Mg, 75.10.Nr

Keywords:

## I. INTRODUCTION

In this paper we examine the scaling behavior of minimum-energy domain wall (MEDW) excitations for two-dimensional Ising spin glasses. Spin glasses are a prototypical model [1, 2, 3, 4] for systems with quenched disorder in statistical mechanics. In general, despite more than two decades of intensive research, many properties of spin glasses, especially in finite dimensions, are still not well understood. The situation is slightly better for two-dimensional spin glasses, because it is now widely accepted that no ordered phase for finite temperatures exists [5, 6, 7, 8, 9]. For  $d = 2$  the behavior can be described well by a zero-temperature droplet scaling (DS) approach [10, 11, 12]. Within this approach, the excitation energy of domain walls and other excitations scales like  $\Delta E \sim L^\theta$ , where  $L$  is the system size and  $\theta$  is referred to as stiffness exponent. Within DS,  $\theta$  is assumed to be universal for all types of excitations. Further, the surface of an excitation is assumed to display a scaling that is characterized by a fractal dimension  $d_f$ .

For Gaussian disorder of the interactions, prior investigations of domain walls resulted in estimates for the stiffness exponent  $\theta = -0.287(4)$  [7, 13] and the values for the MEDW fractal dimension listed in Tab. I. For this model, it was recently indeed confirmed [14, 15] that the value of  $\theta$  is the same also for other types of excitations. Recent studies suggested that such domain walls are governed by stochastic Loewner evolution (SLE) processes [16, 17]. Within conformal-field theory, it seems possible to relate the MEDW fractal dimension  $d_f$  to the stiffness exponent  $\theta$  via

$$d_f - 1 = 3/[4(3 + \theta)]. \quad (1)$$

Note that for a wide range of values of  $\theta$ , one gets very similar results for the fractal dimension, e.g.  $d_f(\theta = -0.2) = 1.268$ , while  $d_f(\theta = -0.3) = 1.278$ . Hence, a

high accuracy is needed to verify whether the proposed relation is compatible with the data. Note that the error bars of the previous results for  $d_f$  are typically of order  $10^{-2}$  or larger, i.e. ten times larger than our high-precision result. Also, we reach much larger system sizes than previous work (also a bit larger than the recent study in Ref. [18], which is anyway for a different lattice type), which also reduces systematic errors due to unknown corrections to scaling.

Reference	$d_f$	Geom.	System	Alg.
Middleton [19]	1.25(1)	tr	$256 \times 256$	M
Bray/Moore [20]	1.26(3)	sq	$12 \times 13$	TM
Kawashima/Aoki [21]	1.28(2)	sq	$48 \times 48$	M
Bernard <i>et. al.</i> [17]	1.28(1)	tr	$720 \times 360$	M
Rieger <i>et. al.</i> [5]	1.34(10)	sq	$30 \times 30$	BC
Palassini/Young [22]	1.30(8)	sq	$30 \times 30$	BC
Weigel/Johnston [18]	1.273(3)	hex	$256 \times 256$	M

TABLE I: Previous results on the fractal dimension of MEDWs arising from Gaussian disorder in two dimensions. From left to right: Reference, estimate value of the fractal dimension  $d_f$ , geometry of the system (sq: square lattice, tr: triangular lattice, hex: hexagonal lattice), largest system studied and numerical algorithm used, for details see cited references (M = matching approaches, TM = ( $T = 0$ ) transfer matrix method, BC = branch-and-cut algorithm).

For the  $\pm J$ -model it was found that the MEDW energy saturates at a nonzero value for large system sizes [7, 23], which means  $\theta = 0$ . It exhibits a high degeneracy of ground states (GSs) and thus allows for numerous MEDWs, e.g. varying in length, see Fig. 1. As a result, the concept of a MEDW is not clear-cut. Referring to this model, the SLE scaling relation above cannot be adopted. Recent attempts to capture the frac-

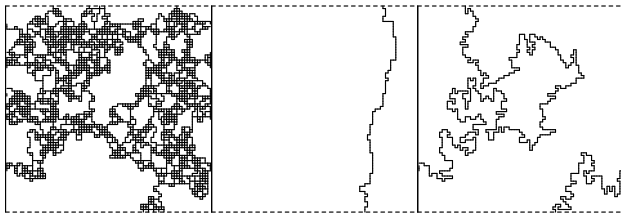


FIG. 1: For the  $\pm J$  model, a high degeneracy appears. Hence, for each of the GSs, many MEDWs separating the left and right border exist, which having all the same minimum energy. Left: many MEDWs for a sample system of size  $L = 80$ , middle (right): corresponding  $\pm J$ -min ( $\pm J$ -max) MEDW. Dashed lines denote free boundary conditions, solid lines indicate periodic boundary conditions.

tal properties of typical MEDWs arising from bimodal disorder concluded with values  $d_f = 1.30(1)$  [24] and  $d_f = 1.283(11)$  [18]. Nevertheless, in these works there is still no systematics concerning the selection of a representative MEDW, as mentioned in Ref. [18]. The sampling of the domain walls is not controlled, hence different configurations having the same energy do *not* contribute to the results with the same weight. Currently, no fast algorithm is known which allows to sample the degenerate GSs and/or MEDWs correctly. For a correct sampling, all degenerate configurations must contribute to the results with the same weight or probability. So far this can be done only for small systems through enumeration of all GS configurations [25]. Some investigations use a scaling relation from droplet theory [11], which quotes that the variance of the DW entropy should also scale like a power law with the system size, with the same exponent  $d_f$ . In a recent investigation based on this relation for square lattices of size up to  $L = 256$  [26] a value of  $d_f = 1.090(8)$  for  $24 \leq L \leq 96$  and  $d_f = 1.30(3)$  for  $L \geq 96$  was reported. On the other hand, other studies on the scaling behavior of the MEDW entropy [27, 28] suggested that the behavior of zero-energy DWs is not consistent with the droplet scaling picture. In this context it was proposed to treat MEDWs of zero and non zero energies as distinct classes. These findings were supported by calculations for square lattices as well as for an aspect ratio different from unity. Hence, due to these results, a direct determination of the MEDW fractal dimension appears to be preferable.

So as to shed further light on their fractal properties, we investigate MEDWs originating from bimodal and Gaussian disorder. We use exact algorithms [29], which allow to obtain the domain walls with the true lowest energy. Here, we describe a novel approach to the problem of finding MEDWs in terms of minimum-weight paths, detailed in the forthcoming section. It allows to put a lower bound and an upper estimate on the scaling behavior of MEDWs and it might further provide a sound basis to investigate the scaling behavior of typical MEDWs for the  $\pm J$  model, similar to the random-field Ising model, where all ground states can be represented by a certain

graph [30], which should allow for unbiased sampling of ground states. Moreover, the corresponding picture of minimum-weight paths on undirected graphs, that allow for negative edge weights, leads to a percolation problem that appears to be interesting on its own, i.e. seems to be in a new universality class [31]. For the bimodal system, to avoid aforementioned problems of sampling correctly equivalent MEDWs of different length, we ask for those MEDWs with extremal lengths, bearing a true lower bound and an upper estimate  $1.095(2) < d_f < 1.395(3)$  in case of bimodal disorder. In addition, for the Gaussian system, we study square lattices with a large number of samples and much larger system sizes than previously studied in the literature, yielding a result for the fractal dimension  $d_f = 1.274(2)$ , which has an enhanced precision compared to the results shown in Tab. I and compares well with the value  $d_f^{\text{SLE}} = 1.2764(4)$  obtained via inserting  $\theta = -0.287(4)$  into Eq. (1). Finally, we also study for the first time the scaling-behavior of the domain-wall roughness and of the distributions of domain-wall length and width.

The paper is organized as follows. In the next section, we present the details of the model and the numerical algorithms we have applied. In the third section, we show all our results. We conclude with a summary in section four.

## II. MODEL AND METHOD

In the framework of this paper, we present GS calculations of two-dimensional Ising spin glasses with nearest-neighbor interactions. The model consists of  $N = L \times L$  spins  $\sigma = (\sigma_1, \dots, \sigma_N)$  with  $\sigma_i = \pm 1$  located on the sites of a square lattice. The energy is given by the Edwards-Anderson Hamiltonian

$$H(\sigma) = - \sum_{\langle i,j \rangle} J_{ij} \sigma_i \sigma_j, \quad (2)$$

where the sum runs over all pairs of neighboring spins, with periodic boundary conditions (BCs) in the  $x$ -direction and open BCs in the  $y$ -direction. The bonds  $J_{ij}$  are quenched random variables drawn according to a given disorder distribution. They can take either sign and thus lead to competing interactions among the spins. Here, we consider two kinds of disorder distributions: (i) Gaussian with zero mean and variance one, and (ii) a bimodal distribution  $J_{ij} = \pm 1$  with equal probability ( $\pm J$  model).

In this work, we study minimum-energy domain walls, which are certain excitations that are defined, for each realization of the disorder, relative to two spin configurations:  $\sigma$  is a ground state with respect to periodic BCs ( $x$ -direction) and  $\sigma^{\text{AP}}$ , a GS obtained for antiperiodic BCs. One can realize antiperiodic BCs by inverting the signs of one column of spins, described by the Hamiltonian  $H^{\text{AP}}(\sigma)$ . Considering both spin configurations, MEDWs separate two regions on the spin lattice:

one, where the spins have the same orientation in both GSs and another, where the spins have different orientations regarding the two GSs. In the above periodic-antiperiodic setup, one domain wall will run through the inverted bonds. This straight-line domain wall is not of interest to us. Instead, we are interested in the MEDW which consists of those bonds that are fulfilled in exactly one of the two GSs. Hence, the energy of the MEDW is given by  $H^{\text{AP}}(\sigma^{\text{AP}}) - H(\sigma)$  and this is the minimum energy among all the system-spanning (top-down) DWs. This MEDW feature is an integral part of our attempt to study the problem of finding MEDWs in terms of a minimum-weight path problem.

First, we will now outline the main steps of our algorithm and elaborate on them afterwards. The algorithm can be decomposed into the following 4 steps: For each given realization of the bond disorder (i) find a GS spin configuration consistent with periodic BCs in  $x$ -direction, (ii) determine all possible MEDW segments on the dual of the spin lattice, (iii) map the problem to an auxiliary graph and find a minimum weighted perfect matching (MWPM), (iv) interpret the MWPM as minimum-weight path on the dual graph that represents a MEDW on the spin lattice.

Step (i): For the calculation of the GS  $\sigma$ , we apply an exact matching algorithm that works for planar systems without external fields, e.g. a square lattice with periodic BCs in at most one direction. For this purpose, the system has to be represented by its frustrated plaquettes and paths connecting those pairwise. Finding a minimum-weighted perfect matching on the graph of frustrated plaquettes then corresponds to finding a GS spin configuration on the spin lattice. For a comprehensive description, see Refs. [29, 32, 33, 34]. This well established method yields the exact GS of the frustrated spin-glass model and allows to explore large system sizes, easily more than  $10^5$  spins, within a reasonable amount of computing time.

Step (ii): Once the GS is obtained we construct the dual of the spin lattice as weighted graph  $G = (V, E, \omega)$ . The vertices  $V$  are given by all the distinct plaquettes on the spin lattice and edges  $e \in E$  connect vertices, where the corresponding plaquettes have a bond in common, i.e. the edge crosses the corresponding bond, see Fig. 2. Note that there are two “extra” vertices above and below the system. Further, a weight (or distance)  $\omega(e)$  is assigned to each edge of  $G$ , equal to the amount of energy that it would contribute to a MEDW, i.e.  $\omega(e) = 2J_{ij}\sigma_i\sigma_j$  for  $\langle i, j \rangle$  being the bond crossed by the edge  $e$ ,  $\sigma$  being the GS obtained in step (i). In this sense, the dual graph comprises all possible MEDW segments. A DW is a path in the dual graph and the energy of a DW is the sum of the weight of all segments being part of a DW. The GS property of the spin configuration has an impact on the weight distribution of  $G$ . There are negative edge weights but one cannot identify loops with negative weight. This will be of importance later. In summary, a MEDW is a path with minimum weight joining the extra vertices of

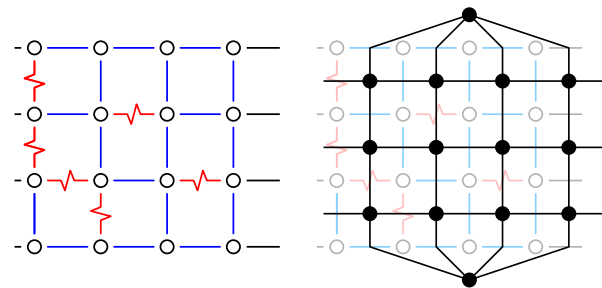


FIG. 2: (color online) Construction of the dual of the spin lattice. Left: Spin lattice with periodic BCs in the horizontal direction (denoted by black bonds at the left and right column) and free BCs along the top and bottom boundary. The sites are denoted by the circles, the bonds are the straight and jagged lines. For clarity, spins are not drawn. Right: Vertices and edges of the dual graph. Note that two extra vertices on top and at the bottom are introduced to account for the free BCs.

$G$ .

Step (iii): Since  $G$  is an undirected graph that allows for negative edge weights, it requires matching techniques to construct minimum-weight paths [35]. Following this reference, we therefore map the problem onto an auxiliary graph  $G_A$  obtained from the dual graph by the following procedure: For every vertex  $i$  in the dual graph (except the two extra vertices above and below the lattice)  $G_A$  contains a pair of “duplicate” vertices  $i^{(a)}, i^{(b)}$  which are connected by an edge of zero weight. Furthermore for every edge  $e = (i, j)$  in the dual graph, two additional vertices  $a^{(i,j)}, b^{(i,j)}$  are introduced which are connected by an edge  $(a^{(i,j)}, b^{(i,j)})$ . One of these two vertices is connected to the duplicate vertices representing  $i$  (e.g. via edges  $(a^{(i,j)}, i^{(a)}), (a^{(i,j)}, i^{(b)})$ ), the other one to the duplicate vertices representing  $j$  (via edges  $(b^{(i,j)}, j^{(a)}), (b^{(i,j)}, j^{(b)})$ ). All edge weights are zero, except for the edges connecting one of the additional vertices to the duplicates it is connected to, which carry the weight of  $\omega(e)$ , see Fig. 3. We then apply an algorithm from the LEDA [36, 37] library to obtain a MWPM on  $G_A$ .

Step (iv): The MWPM consists of a certain subset of the edges of  $G_A$ . In order to interpret it as minimum-weight path on the dual graph, one has [35] to perform a partial inverse transformation of step (iii). This means, we merge all adjacent vertices with the same type, i.e. all pairs  $i^{(a)}, i^{(b)}$  of “duplicate” vertices and all pairs  $a^{(i,j)}, b^{(i,j)}$  of additional vertices. The edges in the matching which are between vertices of the same type disappear, while the other edges “remain”, which means each edge  $(a/b^{(i,j)}, i/j^{(a)/(b)})$  becomes an edge  $(a/b^{(i,j)}, i/j)$ . Thus, some of the edges contained in the matching disappear, while the remaining ones form (for a proof and further details see Ref. 35) a path of minimal weight, connecting the extra vertices of  $G$ . This path in turn corresponds to the MEDW on the spin lattice.

One advantage of the above procedure, in comparison with computing the GSs for periodic and antiperiodic

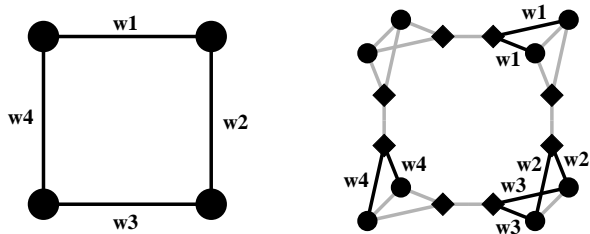


FIG. 3: Construction of the auxiliary graph: Every connected pair of vertices on the dual is replaced by a construct of 6 vertices and 7 edges. This transformation is illustrated for 4 edges depicted on the left, with weights  $w_1$ ,  $w_2$ ,  $w_3$  and  $w_4$ . After the transformation the gray edges carry zero weight and the black edges carry the same weight as the original edge on the dual. For an illustrative purpose the vertices are divided into round and squared ones.

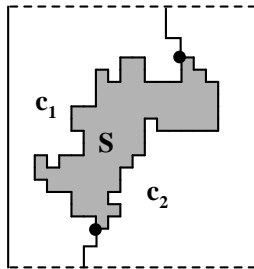


FIG. 4: Extension of the algorithm: subpath  $c_1$ , replacement path  $c_2$  and pivoting spin cluster  $S$  that might be flipped in order to improve a MEDW regarding its length.

boundary conditions, is that it yields an explicit representation of a MEDW. This allows to determine quantities like length/roughness scaling exponents directly. The main advantage is related to the  $\pm J$ -model. There, it is possible to lift the degeneracy among the MEDWs. One can obtain MEDWs with an exactly minimum and a maximal (i.e. not maximum) number of segments, i.e. exactly shortest and very long MEDWs.

First, the slight modification  $\omega(e) \rightarrow \omega(e) + \epsilon$  ( $\epsilon > 0$ ) represents a negative feedback for the inclusion of path segments, hence the MEDW will be among all MEDWs that one which includes a minimal number of path segments, i.e. a shortest MEDW. The value of  $\epsilon$  must be small enough to maintain the minimum-weight path structure on the dual graph, e.g.  $\epsilon < 1/|E|$ . This modification is referred to as  $\pm J$ -min. The modification  $\omega(e) \rightarrow \omega(e) - \epsilon$  represents a positive feedback for the inclusion of path segments to the MEDW. Hence, the MEDW obtained in this way will be, among all MEDWs, one which will include a large number of path segments. This is referred to as  $\pm J$ -max. However, in the latter case arises a serious difficulty: the weight distribution may allow for loops with negative weights now, and, due to the nature of the MWPM problem, the algorithm returns a minimum-weight path in the presence of loops with negative weight. Hence, only the total number of

segments of the minimum-weight path together with all loops (of zero energy in the unmodified graph) is maximized, not the number of segments of a minimum-weight path alone. So we are only able to obtain a lower bound on the longest MEDWs via using the  $\pm J$ -max approach. Note that obtaining the true longest minimum-weight MEDWs is an NP-hard problem, which means that only algorithms are known, where the running time increases exponentially with the number  $N$  of spins.

Another drawback is the fact, that the MEDW depends on the spin configuration determined in step (i). To get really the shortest MEDWs ( $\pm J$ -min2), we therefore allow the algorithm to change the GS, if this leads to a shortening of the MEDW. The basic idea is that different GSs differ by a finite number of zero-energy clusters of reversed spins. We are only interested in clusters, where part of the boundary coincides with a MEDW, which lead to a different MEDW of the same energy when flipping the cluster. Note that also the edges connecting to the two extra nodes are considered here as part of the MEDW, hence a flip of one or several zero-energy clusters might lead to another MEDW which has nothing in common with the starting MEDW. Technically, we look for the shortest MEDWs by finding replacement paths for certain subpaths of the MEDW, depicted in Fig. 4. Firstly, one has to find a subpath  $c_1$  of the MEDW with weight  $\omega(c_1) < 0$ . If there is a replacement path  $c_2$  with  $\omega(c_2) = |\omega(c_1)|$  and if  $\text{len}(c_2) < \text{len}(c_1)$  flip the cluster of spins surrounded by  $c_1$  and  $c_2$  to yield a shorter path with minimum weight. This is repeated until no such shortening of the MEDW is possible any more. Since the flipping of the spin cluster does not cost energy (the loops  $c_1, c_2$  are zero-energy loop in the unmodified graph), the GS property of the spin configuration is maintained. This latter elaboration of the algorithm is computationally more expensive because we have to consider all possible subpaths  $c_1$  with  $\omega(c_1) < 0$ . This means, we can obtain the true shortest MEDWs, considering all possible GSs, only for small sizes  $L \leq 32$ . For large sizes, we study only the shortest MEDW for the given GS, which was obtained in step (i).

### III. RESULTS

In Fig. 1 we show several MEDWs for a system with  $\pm J$  disorder, one long  $\pm J$ -max MEDW and one shortest  $\pm J$ -min MEDW, respectively. Already from these

	$L < 160$	$L = 160$	$L = 226$	$L = 320$
Gaussian	40000	10000	2800	2000
$\pm J$ -min	40000	40000	20000	10000
$\pm J$ -max	40000	20000	5000	5900

TABLE II: Number of samples investigated for the different system sizes.



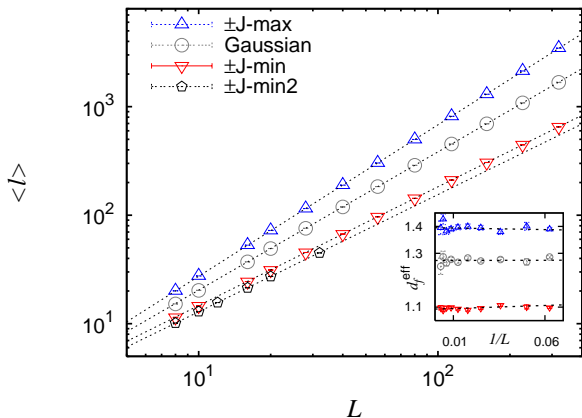


FIG. 5: (color online) Scale dependence of the average MEDW length. Fits to the form  $\langle \ell \rangle \sim L^{d_f}$  (dashed lines) yield the exponents quoted in Tab. III. The inset shows the local slopes for the Gaussian and  $\pm J$ -min(max) MEDWs as function of  $1/L$ , providing comparable values for  $d_f$  but with larger error bars (see text).

samples one can expect an observable difference in their scaling behavior.

We expect the disorder-averaged MEDW length  $\ell$  to scale with the system size according to  $\langle \ell \rangle \sim L^{d_f}$ , where  $\langle \dots \rangle$  denotes the disorder average and  $1 \leq d_f \leq 2$  denotes the fractal dimension of the MEDW. Its roughness  $r$ , given by the difference in the coordinates of its leftmost and rightmost position on the spin lattice, should display the scaling behavior  $\langle r \rangle \sim L^{d_r}$ , with a roughness exponent  $d_r$ . To determine the scaling behavior of the MEDWs, we have studied systems with sizes up to  $L=320$  and averaged over up to 40000 realizations of the disorder, see Tab. II.

In Fig. 5, we show the result for  $\langle \ell \rangle$  as function of system size for the Gaussian disorder and the three cases studied for the  $\pm J$  model. The data can be fitted very well to power laws, the results are shown in Tab. III. As an alternative method, we also estimate the value of the scaling exponent  $d_f$  using the local (successive) slopes of the data points, see also [39]. The results are compatible with the data given in Tab. III, only this procedure leads to a more conservative estimate of the numerical error, leading to the error bars as given in Tab. III.

	$d_f$	$Q$	$d_r$	$Q$
Gaussian	1.274(2)	0.45	1.008(11)	0.40
$\pm J$ -min	1.095(2)	0.27	1.006(6)	0.78
$\pm J$ -max	1.395(3)	0.16	0.993(8)	0.35

TABLE III: Scaling exponents of the mean MEDW length ( $d_f$ ) and its roughness ( $d_r$ ). Fits are restricted to  $L \geq 26$  ( $d_f$ ) and  $L \geq 50$  ( $d_r$ ). The value of  $Q$  gives a measure for the quality of the fit [38].

The estimate for the MEDW fractal dimension in case of a Gaussian distribution of the interaction strengths is in good agreement with earlier results, but has an enhanced precision, see Tab. I. Note that the treatment of large systems reduces the influence of systematic errors due to unknown corrections to scaling, hence providing a very reliable result for  $d_f$ . Further, it is consistent with the result  $d_f^{\text{SLE}} = 1.2764(4)$  predicted by the SLE scaling relation, where we considered  $\theta = -0.287(4)$  from Ref. [13]. For the  $\pm J$ -model we obtained a lower bound  $d_f = 1.095(2)$  that is distinct from 1, indicating that overhangs are still significant for MEDWs with minimal length. Further, the estimate of the upper bound  $d_f = 1.395(3)$  points out that DWs with maximal length are not space-filling. Note that using the past results [18, 24], which are based on an uncontrolled sampling of domain walls, one could *not* exclude these values  $d_f = 1$  and  $d_f = 2$ .

As pointed out in the description of the algorithm, the  $\pm J$ -min value actually overestimates the scaling behavior of MEDWs with minimal length. Therefore we performed calculations with the computationally more expensive algorithm, that allows for a change of the GS spin configuration. We considered system sizes  $L \leq 32$  with up to 3000 samples and subsequent fits were restricted to  $12 \leq L \leq 32$ . Albeit affected by finite size effects, we found  $d_f = 1.080(5)$  ( $Q = 0.40$ ) for the  $\pm J$ -min2 DWs, compared to a value of  $d_f = 1.105(2)$  ( $Q = 0.43$ ) when fitting the results for  $\pm J$ -min MEDWs in the same interval. Hence, minimal-length and true minimum-length MEDWs are very similar, which means that the  $\pm J$ -min MEDWs, where we can obtain results for large sizes, yield a reliable estimate of the behavior of shortest MEDWs.

Also, we analyzed the scaling behavior of MEDWs of different energies for the  $\pm J$ -model, in particular for those which have energies  $E_{\text{DW}} = 0$  or  $E_{\text{DW}} = 2$  (which constitute 96% of all MEDWs, the remaining 4% are  $E_{\text{DW}} = 4, 6, 8, 10$ ). In all cases we find again power-law behavior (not shown) with  $\langle \ell \rangle \sim L^{d_f}$ , the resulting exponents are almost compatible within error bars to the average result above. Note that in recent studies [27, 28] of the DW entropy, contrarily, the behavior of  $E_{\text{DW}} = 0$  and  $E_{\text{DW}} \neq 0$  DWs was very different.

Also for the scaling of the domain-wall roughness with system size, we find a power law behavior, see Fig. 6. The resulting roughness exponents are shown again in Tab. III. The roughness exponents, obtained using local slopes exhibit again larger error bars. Hence, in all cases studied here the roughness exponent appears to be compatible with unity, showing that the width of the MEDWs scales like the extension in  $y$ -direction, as predicted in Ref. [21]. Regarding the roughness, one finds stronger finite-size effects for small  $L$ , where we again have compared minimal-length and true minimum-length MEDWs. Fits to the data in the interval  $16 \leq L \leq 32$  yields  $d_r = 1.101(15)$  ( $Q = 0.75$ ) for the true minimum-length  $\pm J$ -min2 MEDWs and  $d_r = 1.070(2)$  ( $Q = 0.79$ ) for the minimal-length  $\pm J$ -min MEDWs. Hence, minimal-

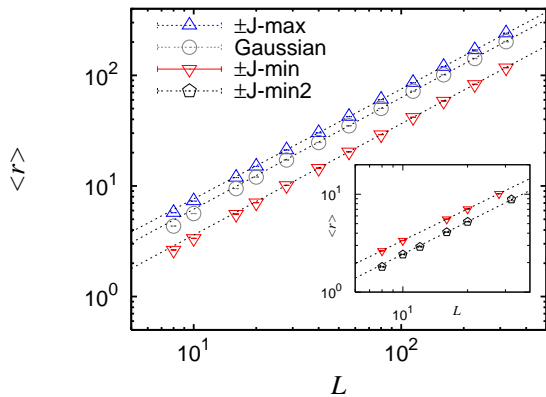


FIG. 6: (color online) Scale dependence of the average MEDW roughness. Fits to the form  $\langle r \rangle \sim L^{d_r}$  for  $L \geq 50$  (dashed lines) yield exponents listed in Tab. III. The inset shows the scaling of  $\pm J$ -min compared to the  $\pm J$ -min2 MEDWs.

length and true minimum-length MEDWs are again very similar, which means that the  $\pm J$ -min MEDWs yield a reliable estimate of the shortest MEDW behavior.

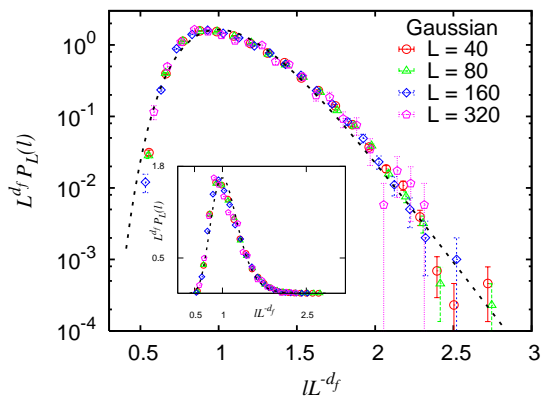


FIG. 7: (color online) Scaling plot of the MEDW length distribution  $P_L(\ell)$  for Gaussian disorder, where the dashed line is a log-normal distribution with mean  $\mu = 1.06(1)$  and standard deviation  $\sigma = 0.24(1)$ , obtained from a fit to the data of  $L = 160$ .

So far, we have analyzed the scaling behavior of mean values, now we turn to the full distributions. The main result is that the distributions  $P_L(\ell)$  of the MEDW length for different system sizes can be related to each other via a simple scaling relation. As can be seen from Fig. 7, rescaling of the length distributions according to  $P_L(\ell) = L^{-d_f} f(\ell L^{-d_f})$  yields a collapse to a master curve. A qualitative similar behavior was found for the scaling of optimal paths in strong and weak disorder [39, 40], the mass distribution of the backbone in critical percolation [41] and regarding undirected minimum-weight paths in 2d lattice graphs, where the effect of isotropically correlated bond weights on the scaling exponents was investigated [42]. Note that the distribution

is peaked close to  $\langle \ell \rangle$ . This holds also for MEDWs subject to  $\pm J$  disorder (not shown), where one can observe an additional even/odd deviation in the distribution of the MEDW lengths. This deviation results in a preferential appearance of domain walls with even length, responsible for defect-energies  $E_{DW} = 0 \pmod{4}$ .

As it turns out, the particular shape of the scaling function is very simple for the case of Gaussian disorder. It is possible to fit the distributions in this case satisfactory by use of log-normal scaling functions.

Fig. 7 shows an example, where the log-normal distribution  $p(x) = \exp[-(\ln(x/\mu))^2/2\sigma^2]/(x\sigma\sqrt{2\pi})$  with  $x = \ell L^{-d_f}$  was fit to the data ( $L = 160$ ), resulting in a mean and standard deviation  $\mu = 1.06(1)$  and  $\sigma = 0.24(1)$ , respectively. This scaling function does not suit the bimodal disorder case. Here, for MEDWs with minimal length, we observe an exponential decay of  $P_L(\ell)$  with increasing  $\ell \geq \langle \ell \rangle$  and estimated the decay exponent  $\alpha = -5.9(2)$  from a fit to the data corresponding to  $L = 320$ . The DWs with maximal length somehow resemble the Gaussian case, but we could not find a meaningful distribution to describe it.

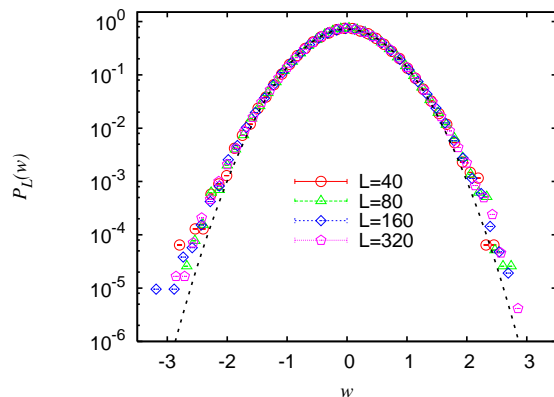


FIG. 8: (color online) Distribution  $P_L(w)$  of weights  $w$  on the MEDW segments for different system sizes  $L$ . The dashed line is a Gaussian distribution with mean  $\mu = -0.0003(40)$  and standard deviation  $\sigma = 0.552(3)$ , obtained from a fit to the data corresponding to  $L = 320$ . Results were averaged over  $10^3$  samples.

Finally, we look at the distribution  $P_L(w)$  of weights  $w$  which comprise the segments along the obtained MEDW for different system sizes, see Fig. 8. Since the segments available to the DWs are a result of a GS calculation, and because each MEDW is the result of another optimization procedure, the behavior is a priori not clear. Clearly, bonds with very negative energy will not occur, because these bonds with a large absolute value will be satisfied in the ground state with high probability, hence yield a positive contribution to the energy of a domain wall. This contributes to a decrease of the width of the distribution  $P_L(w)$ , compared to the underlying disorder distribution. Apart from this effect, the resulting data compares well to a Gaussian with mean 0 and a standard deviation close

to 0.5: from a fit to the data at  $L = 320$ , we have obtained a mean  $\mu = -0.0003(40)$  and a standard deviation  $\sigma = 0.552(3)$ . Note that the distributions do not seem to depend strongly on the system size.

#### IV. SUMMARY

In summary, we have performed GS and DW calculations for 2d Ising spin glasses with short ranged interactions via exact optimization algorithm. Exploring large system sizes, we investigated the fractal properties of MEDWs arising from Gaussian and bimodal disorder.

Our approach is based on a minimum-weight path approach for paths on undirected networks which can have negative edge weights. This allows for a more direct calculation of MEDWs. Presently, in the case of the degenerate  $\pm J$  model, we are able to calculate the shortest and very long paths, which allows to obtain bounds on the fractal properties of the MEDWs. We believe that this approach could serve as a basis for the desired calculation of *typical* DWs for the  $\pm J$  model.

For the  $\pm J$  model we found a lower bound  $d_f = 1.095(2)$ , which is clearly larger than unity, and we estimated an upper bound  $d_f = 1.395(3) < 2$ . These exponents do not change when we analyze the scaling behavior of MEDWs restricted to certain energies. Our results for the length scaling exponent in case of Gaussian disorder  $d_f = 1.274(2)$  is in agreement with prior results but with strongly enhanced precision. Further, it compares well to the result obtained from the recently proposed SLE scaling relation. Furthermore, we found that the full distributions of the MEDW lengths scale with the same fractal exponent  $d_f$ . This behavior was also found

for observables in a different physical context. Finally, the width of the domain wall scales like its height, for all cases considered here.

For later work, one could consider models with a  $T = 0$  transition between a ferromagnetic phase and a spin-glass phase, and study the behavior of the fractal dimensions around this transition. Here, from Eq. (1), one would expect to observe a discontinuous change of the exponents when approaching the transition, because  $\theta$  is expected to be the same everywhere in the spin-glass phase. Furthermore, it would be desirable to be able to sample GSs for the  $\pm J$  model in equilibrium, hence each GS would contribute provably with equal weight/probability to all results. This would allow to determine a fractal dimension of the average domain wall. This value might be related to the energy-scaling exponent  $\theta$  via a relation similar to Eq. (1).

#### Acknowledgments

We would like to thank Ron Fisch, Matthew Hastings and Mike Moore for many valuable discussions. Furthermore, we are grateful to Mike Moore for a critical reading of the manuscript. We obtained financial support from the VolkswagenStiftung (Germany) within the program “Nachwuchsgruppen an Universitäten”. Financial support by the European Community’s Human Potential Program under contract number HPRN-CT-2002-00307, DYGLAGEMEM is also acknowledged. The simulations were performed at the “Gesellschaft für Wissenschaftliche Datenverarbeitung” and the workstation cluster of the “Institute for Theoretical Physics”, both in Göttingen, Germany.

- 
- [1] K. Binder and A. Young, *Rev. Mod. Phys.* **58**, 801 (1986).
  - [2] M. Mézard, G. Parisi, and M. Virasoro, *Spin glass theory and beyond* (World Scientific, Singapore, 1987).
  - [3] K. Fischer and J. Hertz, *Spin Glasses* (Cambridge University Press, Cambridge, 1991).
  - [4] A. Young, ed., *Spin glasses and random fields* (World Scientific, Singapore, 1998).
  - [5] H. Rieger, L. Santen, U. Blasum, M. Diehl, and M. Jünger, *J. Phys. A* **29**, 3939 (1996).
  - [6] N. Kawashima and H. Rieger, *Europhys. Lett.* **39**, 85 (1997).
  - [7] A. K. Hartmann and A. P. Young, *Phys. Rev. B* **64**, 180404 (2001).
  - [8] J. Houdayer, *Eur. Phys. J. B* **22**, 479 (2001).
  - [9] A. C. Carter, A. J. Bray, and M. A. Moore, *Phys. Rev. Lett.* **88**, 077201 (2002).
  - [10] W. L. McMillan, *J. Phys. C* **17**, 3179 (1984).
  - [11] D. S. Fisher and D. A. Huse, *Phys. Rev. B* **38**, 386 (1988).
  - [12] D. S. Fisher and D. A. Huse, *Phys. Rev. Lett.* **56**, 1601 (1986).
  - [13] A. K. Hartmann, A. J. Bray, A. C. Carter, M. A. Moore, and A. P. Young, *Phys. Rev. B* **66**, 224401 (2002).
  - [14] A. K. Hartmann and M. A. Moore, *Phys. Rev. Lett.* **90**, 12720 (2003).
  - [15] A. K. Hartmann and M. A. Moore, *Phys. Rev. B* **69**, 104409 (2004).
  - [16] M. B. H. C. Amoroso, A. K. Hartmann and M. A. Moore, *Phys. Rev. Lett.* **97**, 267202 (2006).
  - [17] D. Bernard, P. Le Doussal, and A. A. Middleton (2006), cond-mat/0611433.
  - [18] M. Weigel and D. Johnston, cond-mat/0701550 (2007).
  - [19] A. A. Middleton, *Phys. Rev. B* **63**, 060202 (2001).
  - [20] A. J. Bray and M. A. Moore, *Phys. Rev. Lett.* **58**, 57 (1987).
  - [21] N. Kawashima and T. Aoki, cond-mat/9911120 (1999).
  - [22] M. Palassini and A. P. Young, *Phys. Rev. B* **60**, R9919 (1999).
  - [23] C. Amoroso, E. Marinari, O. C. Martin, and A. Pagnani, *Phys. Rev. Lett.* **91**, 087201 (2003).
  - [24] F. Roma, S. Risau-Gusman, A. J. Ramirez-Pastor, F. Nieto, and E. E. Vogel, *Phys. Rev. B* **75**, 020402(R) (2006), cond-mat/0607565.
  - [25] J. W. Landry and S. N. Coppersmith, *Phys. Rev. B* **65**, 134404 (2002).

- [26] A. Aromsawa and J. Poulter, arXiv:0704.1186v1 (2007).
- [27] R. Fisch, *J. Stat. Phys.* **125**, 789 (2006).
- [28] R. Fisch, cond-mat/0703137 (2007).
- [29] A. K. Hartmann and H. Rieger, *Optimization Algorithms in Physics* (Wiley-VCH, Weinheim, 2001).
- [30] A. K. Hartmann, *Physica A* **248**, 1 (1998).
- [31] O. Melchert and A. K. Hartmann, in preparation.
- [32] F. Barahona, *J. Phys. A: Math. Gen.* **15**, 3241 (1982).
- [33] I. Bieche, R. Maynard, R. Rammal, and J. P. Uhry, *J. Phys. A: Math. Gen.* **13**, 2553 (1980).
- [34] W. Janke, ed., *Rugged Free Energy Landscapes* (Springer, 2007).
- [35] R. K. Ahuja, T. L. Magnanti, and J. B. Orlin, *Network Flows: Theory, Algorithms, and Applications* (Prentice Hall, 1993), ISBN 013617549X.
- [36] K. Mehlhorn and S. Näher, *LEDA: a platform for combinatorial and geometric computing* (Cambridge University Press, Cambridge, 1999), ISBN 0-521-56329-1.
- [37] K. Mehlhorn and G. Schäfer, in *Algorithm Engineering* (2000), pp. 23–38.
- [38] W. H. Press, S. A. Teukolsky, W. T. Vetterling, and B. P. Flannery, *Numerical Recipes in C* (1992),  $Q$  is the probability that the value of  $\chi^2$  is worse than in the current fit.
- [39] S. V. Buldyrev, S. Havlin, E. López, and H. E. Stanley, *Phys. Rev. E* **70**, 035102 (2004).
- [40] S. V. Buldyrev, S. Havlin, and H. E. Stanley, *Phys. Rev. E* **73**, 036128 (2006).
- [41] M. Barthélémy, S. V. Buldyrev, S. Havlin, and H. E. Stanley, *Phys. Rev. E* **60**, 1123 (1999), cond-mat/9904062.
- [42] R. Schorr and H. Rieger, *Eur. Phys. J. B* **33**, 347 (2003), cond-mat/0212526.